

## MODELLED PHENOMENON OF BURR FORMATION DURING MACHINING

Paweł Preś, Waclaw Skoczyński

Wroclaw University of Technology, Department of Machine Tools and Mechatronic Systems  
Łukasiewicza Street 5, 50-371 Wrocław, Poland  
tel.: +71 320 28 81

e-mail: pawel.pres@pwr.wroc.pl, waclaw.skoczynski@pwr.wroc.pl

### Abstract

*A model of burr formation on the edge of the workpiece in the course of machining is presented. The material being machined, the cutting tool and the machining parameters were modelled. Material properties and type of its deformations have been modelled with the use of a constitutive Johnson - Cook model. Material damage initiation criteria and associated damage evolution have been modelled with the use of the ductile damage and the Johnson-Cook damage initiation criterion. Simulations of the machining process for different depths of cut were carried out. The real burr formation presented by Hashimura was compared with the modelled one. The influence of the cutting parameters on the form and size of burr has been analysed. Calculations have been realised utilising finite element method with the use of nonlinear analysis in ABAQUS/Explicit environment. Based on simulation results, the assessment of the form and size of burr has been made. Burr height was used to evaluate its size, which was derived according to ISO 13715 standard. The goal was to obtain a model that reliably reflects the behaviour of material during machining, with particular emphasis on supporting the creation of cutting phenomenon of burr formation. The results of simulation and computational analysis confirmed that the model reflects the real behaviour of the material.*

**Keywords:** burr formation, finite element simulation, cutting, 2D numerical model

### 1. Introduction

Burr formation accompanies many production processes. It commonly occurs during machining. Problems relating to burr formation, prevention and removal are particularly critical in automated manufacturing. Burrs forming on the workpiece edge directly affect the quality evaluation of the product. Their presence may disturb the proper functioning of the parts, accelerate wear and complicate assembly or even make the latter impossible. Unproductive burr removal operations may amount to as much as 15% of the production costs. In recent years, there has been a growing interest in methods of minimizing burrs. Burr formation is a complicated phenomenon. Many factors determine the size and form of burrs. The key factors include depth of cut, cutting speed, rate of feed, material properties, cutting tool geometry and tool path shape [1-3].

The aim of this research was to develop a fundamental model of burr formation during machining. The Abaqus/Explicit software package was used for this purpose. The computations were based on the dynamic displacement analysis. The simulation results were compared with the real burr formation phenomenon schematically presented by Hashimura [4]. The effect of selected cutting parameters on the size and form of burrs was examined.

### 2. Burr formation phenomenon

A burr can be defined as an undesirable part of the product, clearly deviating from its surface, formed in the course of the manufacturing process. The burr has a much smaller volume than the product volume. In most cases, during machining a burr forms as a result of the action of the cutting forces preventing chip formation through the deformation of some of the material on the workpiece edge [5].

The mechanism of the real burr formation phenomenon, developed by Hashimura [4], is shown in Fig. 1. In the course of machine cutting the zone of elastic deformations and then the zone of plastic deformations visibly, expand as the distance of the tool from the edge of the material being machined changes.

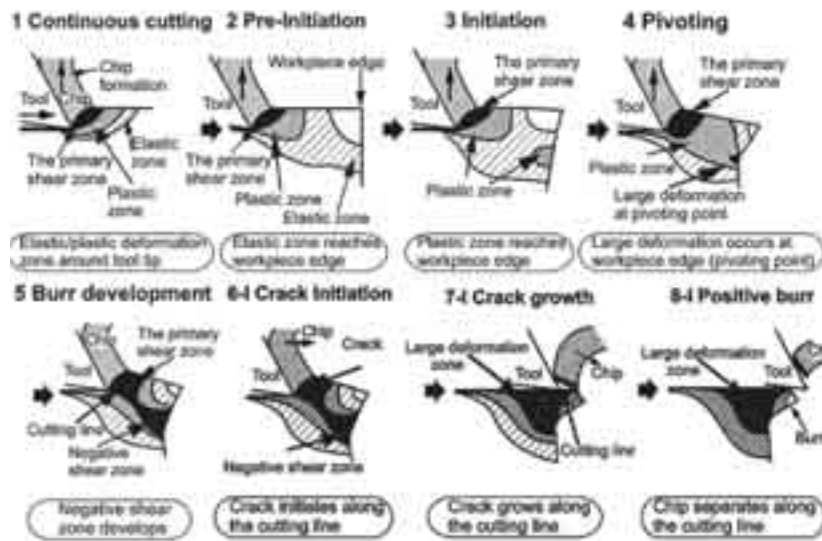


Fig. 1. Schematic illustrating burr formation [4]

A point of rotation appears below the edge of the workpiece. The material at the edge of the workpiece, particularly around the rotation point, undergoes strong plastic deformation and a crack is initiated. As the crack propagates along the plane of shear, a chip separates from the material and a burr forms on the product's edge.

### 3. Model of cutting process

The cutting process was modelled using the Abaqus/Explicit package, four-node finite elements CPE4RT and the arbitrary Lagrangian-Eulerian ALE adaptive mesh technique (to keep the ordered character of the finite element mesh). An equal distance between the nodes was maintained during the discretization of the workpiece model. The edges of the workpiece constituted the boundaries of the area to which the ALE adaptive mesh domain technique was applied.

Figure 2 shows the workpiece geometry, the tool geometry and the prescribed boundary conditions. The material being machined was fixed using the base edge. The nodes on the edge of the workpiece edge were deprived of the ability to displace along axes X and Y. The left and right sides of the material to be machined were fixed in such a way that the material could deform freely and a burr could form. In the cutting process model, the tool, undergoing deformation, would move along axis X. The nodes on the two edges forming the outline of the cutting tool were deprived the ability to displace along axis Y. The tool rake angle was  $\gamma_0 = 5^\circ$  and the tool orthogonal clearance angle was  $\alpha = 5^\circ$ . The corner radius amounted to 0.04 mm.

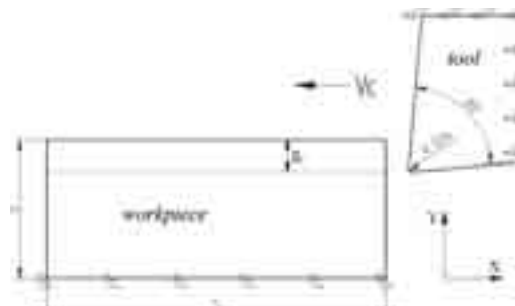


Fig. 2. Boundary conditions

In this research, higher-strength steel C45 was assumed as the machined material. The dependence of the machined material's physical properties on temperature was taken into account in numerical modelling. The values of the Poisson ratio, the Young modulus, density, thermal conductivity, thermal expansion and specific heat were given for a temperature range of 20-700°C.

The behaviour of the material in the course of machining was modelled using the Johnson-Cook constitutive laws. Two deformation material failure criteria resulting in chip separation from the material were implemented. Conditions, the fulfilment of which results in the loss of load capacity, were defined. Elements satisfying the failure criteria would be removed from the simulation.

The Johnson-Cook constitutive model equation (1) has the form [6]:

$$\bar{\sigma} = [A + B(\bar{\varepsilon})^n][1 + C \ln \frac{\dot{\varepsilon}}{\dot{\varepsilon}_0}][1 - \hat{\theta}^m], \quad (1)$$

where:

$\bar{\sigma}$  - reduced flow stress according to Huber-Mises-Hencky for a nonzero strain rate,

$\bar{\varepsilon}$  - reduced plastic strain,

$\dot{\varepsilon}$  - a reduced strain rate,

$\dot{\varepsilon}_0$  - a reference strain rate equal to 1 s<sup>-1</sup>,

A - the initial yield point at a strain rate of 1 s<sup>-1</sup> at transition temperature ( $\theta$ ),

B - a modulus of strain hardening,

n - a strain-hardening exponent,

C - a strain rate coefficient,

m - a thermal softening exponent,

$\hat{\theta}$  - dimensionless temperature.

The dimensionless value of temperature  $\hat{\theta}$  is assumed as follows (2):

$$\hat{\theta} = \begin{cases} 0 & \text{for } \theta < \theta_{trans}, \\ \frac{\theta - \theta_{trans}}{\theta_{melt} - \theta_{trans}} & \text{for } \theta_{trans} < \theta < \theta_{melt}, \\ 1 & \text{for } \theta > \theta_{melt}, \end{cases} \quad (2)$$

$\theta$  - the current temperature,  $\theta_{trans}$  - the transition temperature,  $\theta_{melt}$  - the softening point.

The first part of the Johnson-Cook model equation (1):  $[A + B(\bar{\varepsilon})^n]$  describes the stress-strain dependence for the reference strain rate of 1 s<sup>-1</sup> and transition temperature  $\hat{\theta} = 0$ . Expression  $[1 + C \ln \frac{\dot{\varepsilon}}{\dot{\varepsilon}_0}]$  represents the effect of the cutting speed on the deformation mechanism. The last part of the model:  $[1 - \hat{\theta}^m]$  takes into account the thermal softening effect at high temperature.

Tab. 1. Model parameters and Johnson-Cook failure criterion [7]

Initial yield point	Strain-hardening modulus	Strain rate coefficient	Strain-hardening exponent	Thermal softening exponent	Softening temperature
A [MPa]	B [MPa]	C	n	m	T <sub>melt</sub> [ °C]
553	600	0.021	0.234	1	1538
Material failure parameters					Reference strain rate
d <sub>1</sub>	d <sub>2</sub>	d <sub>3</sub>	d <sub>4</sub>	d <sub>5</sub>	$\dot{\varepsilon}_0$
0.06	3.31	-1.96	0.0018	0.58	0.001

The first of the implemented material failure models is based on the value of reduced plastic strain value  $\bar{\varepsilon}_f^{pl}$ . This dependence (3) can be expressed as follows [8]:

$$\omega = \sum \left( \frac{\Delta \bar{\varepsilon}^{pl}}{\bar{\varepsilon}_f^{pl}} \right), \quad (3)$$

where:

$\Delta \bar{\varepsilon}^{pl}$  – an increment in reduced plastic strain,

$\bar{\varepsilon}_f^{pl}$  – reduced plastic strain at the moment of failure.

The above model is a special case of the ductile criterion. A finite element loses its load-bearing capacity when failure criterion  $\omega$  is equal to 1 ( $\omega = 1$ ). For the Johnson-Cook material failure model the reduced plastic strain at the instant of material failure depends on dimensionless strain rate  $\frac{\dot{\varepsilon}}{\dot{\varepsilon}_0}$ , triaxial stress  $\eta = -\frac{p}{q}$  (where  $p$  – averaged normal stress and  $q$  – reduced Huber stress) and dimensionless temperature  $\hat{\theta}$  (defined earlier in the Johnson-Cook constitutive equation). The relations presented above are independent of each other.

For the Johnson-Cook failure criterion the reduced plastic strain is calculated from the relation (4):

$$\bar{\varepsilon}_f^{pl} = [d_1 + d_2 \exp(d_3 \eta)] [1 + d_4 \ln \frac{\dot{\varepsilon}^{pl}}{\dot{\varepsilon}_0}] (1 + d_5 \hat{\theta}), \quad (4)$$

where:  $d_1 - d_5$  – material failure parameters.

The other failure criterion, which was presented in [8, 9], is connected with the nucleation, growth and merging of small voids in the material. The criterion (5) assumes that at the beginning of material failure reduced strain  $\bar{\varepsilon}_D^{pl}$  depends on the triaxial stress and the strain rate:

$$\bar{\varepsilon}_D^{pl} = f(\eta, \dot{\varepsilon}^{pl}). \quad (5)$$

The reduced strain at the instant of failure is calculated from the relation(6):

$$\bar{\varepsilon}_D^{pl} = \frac{\varepsilon_T^+ \sinh[c(\eta^- - \eta) + \varepsilon_T^- \sinh[c(\eta - \eta^+)]]}{\sinh[c(\eta^- - \eta^+)]}, \quad (6)$$

where:

$\eta^-$ ,  $\eta^+$  – triaxial stress for compression and triaxial stress for tension

$\varepsilon_T^+$ ,  $\varepsilon_T^-$  – reduced strain at the instant of failure for respectively uniform two-axial tension and compression,

$c$  – a parameter dependent on the state of stress.

Failure is initiated once the following criterion (7) is fulfilled:

$$\omega_D = \int \frac{d\bar{\varepsilon}^{pl}}{\bar{\varepsilon}_D^{pl}(\eta, \dot{\varepsilon}^{pl})} = 1, \quad (7)$$

where:  $\omega_D$  – a state variable, monotonically increasing with plastic strain.

The two strain criteria of material failure and identical values of the maximum plastic elongation were used. Ultimately, the effect of the global Johnson-Cook criterion and the local ductile criterion (responsible for exclusively the material cracking resulting in the formation of a burr) was obtained.

#### 4. Simulation of machining process

The modelled process was used to simulate machining. Cutting speed  $v_c$  amounted to

240 m/min. Machining was done for four cut depths: 0.1, 0.25, 0.50 and 0.75 mm. The strongly nonlinear character of the modelled process and the effect of temperature variation (due to the large deformations of the machined material and to the friction between the cutting tool and the material being machined) were taken into account in the simulation. The assumed friction coefficient values on the face were interrelated with normal stress  $\sigma_k$ . Friction coefficient  $\mu$  would decrease as normal stress increased [10]. In addition, the maximum shearing stress was determined.

The height of the burr formed in the process of machining was measured according to standard ISO 13715. The burr height was measured perpendicularly to the edge of the workpiece.

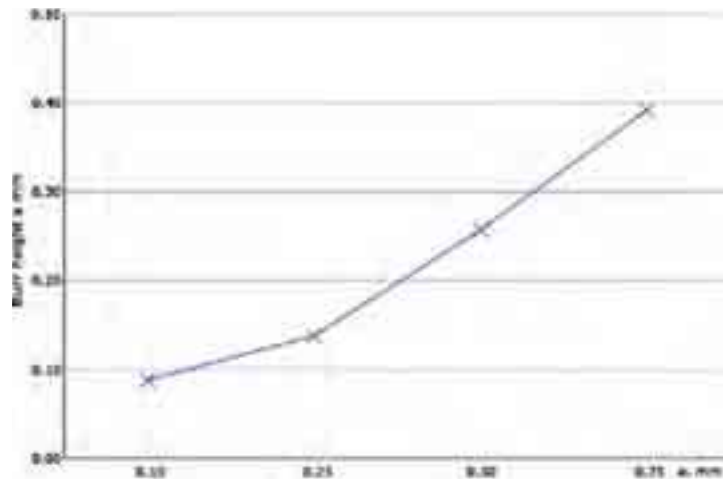


Fig. 3. Burr height depending on depth of cut

The burr formation process worked out on the basis of the results obtained using the Abaqus/Explicit software package is shown in Fig. 4.

A comparison of the schematic proposed by Hashimura [4] (Fig. 1) with the simulation results shows that the described mechanism resulting in the formation of a burr on the edge the workpiece being machined occurs in the course of the modelled machining process. In addition, the next stages, which occur in the real burr formation process, are reflected in the modelled process.

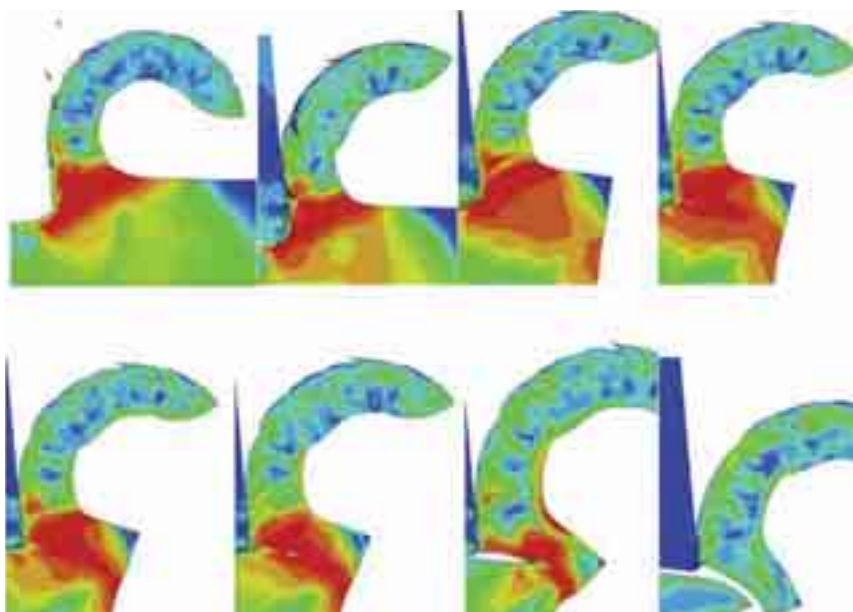


Fig. 4. Simulation of burr formation for cut depth  $a_p = 0.25$  mm and cutting speed  $v_c = 240$  m/min

## 5. Conclusion

Thanks to the state-of-the art computing techniques real manufacturing processes can be increasingly more accurately simulated. On the basis of the simulations and their analysis it can be concluded that:

- the principal aim – a preliminary model of burr formation on the edge of the machined workpiece – has been achieved,
- the stages in burr formation, described in the literature, are accurately represented in the simulation of the modelled machining process,
- because of the adopted two-dimensional geometry, the modelled process in a rather simplified way reflects the real machining process,
- further work on the machining process model, focusing on the way the material undergoes deformation, should result in practical conclusions leading to burr minimization.

## Acknowledgements

The computations were performed on the computers of the Wrocław Centre of Networking and Supercomputing (<http://www.wcss.wroc.pl>), computing grant no. 178.

## References

- [1] Dornfeld, D., Park, W. I., *A study of Burr Formation Process Using the Finite Element Method, Part (II)*, Journal of Engineering Materials and Technology, 122, pp. 229-237, 2002.
- [2] Aurich, J. C., Arrazola, P. J., Dornfeld, D., Franke, V., Leitz, L., Min, S., *Burrs – Analysis, control and removal*, CIRP Annals – Manufacturing Technology, 58, pp. 519-542, 2009.
- [3] Dornfeld, D., *Strategies for Preventing and Minimizing Burr Formation*, CIRP HPC conference in Aachen, Germany, <http://escholarship.org/uc/item/2239m1ns>, 2004.
- [4] Hashimura, M., Hassamont, J., Dornfeld, D., *Effect of In-plane Exit Angle and Rake Angles on Burr Height and Thickness in Face Milling Operation*, Journal of Manufacturing Science and Engineering 121, pp. 13-19, 1999.
- [5] Avila, M., Garder, J., Reich-Wesier, C., Tripanthi, S., Vijayaraghanvan, A., Dornfeld, D., *Strategies for Burr Minimalization and Cleanability in Aerospace and Automotive Manufacturing*, SAE Transactions Journal of Aerospace, 114, pp. 1073-1082, 2005.
- [6] Cook, H. W., Johnson, G. R., *A constitutive model and data for metals subjected to large strains, high strain rates and high temperatures*, Proceedings of Seventh International Symposium on Ballistic, 541, The Hague, The Netherlands, 1983.
- [7] Duan, C. Z., Dou, T., Cai, Y. J., Li, Y. Y., *Finite element simulation and experiment of chip formation process during High Speed Machining of AISI 1045 hardened steel*, International Journal of Recent Trends in Engineering, 5, pp. 46-50, 2009.
- [8] Abaqus 6.9EF software documentation (in Polish).
- [9] Hoopture, H., Gese, H., Dell, H., Werner, H., *A comprehensive failure model for crashworthiness simulation of aluminium extrusions*, International Journal of Crashworthiness, 9, 5, pp. 449-464, 2004.
- [10] Grzesik, W., *Fundamentals of the machining of constructional materials*, WNT, Warsaw 2010.